



Published in final edited form as:

Diabetologia. 2016 January ; 59(1): 151–160. doi:10.1007/s00125-015-3778-2.

Sirtuin 6 regulates glucose-stimulated insulin secretion in mouse pancreatic beta cells

Xiwen Xiong¹, Gaihong Wang¹, Rongya Tao¹, Pengfei Wu², Tatsuyoshi Kono³, Kevin Li⁴, Wen-Xing Ding⁴, Xin Tong^{3,5}, Sarah A. Tersey⁶, Robert A. Harris^{1,2}, Raghavendra G. Mirmira⁶, Carmella Evans-Molina^{2,3,5}, and X. Charlie Dong^{1,*}

¹Department of Biochemistry and Molecular Biology, Indiana University School of Medicine, 635 Barnhill Drive, MS1021D, Indianapolis, IN 46202, USA

²Richard Roudebush Veterans Affairs Medical Center, Indianapolis, IN, USA

³Department of Medicine, Indiana University School of Medicine, Indianapolis, IN, USA

⁴Department of Pharmacology, Toxicology and Therapeutics, University of Kansas, Kansas City, KS, USA

⁵Department of Cellular and Integrative Physiology, Indiana University School of Medicine, Indianapolis, IN, USA

⁶Department of Pediatrics, Indiana University School of Medicine, Indianapolis, IN, USA

Abstract

Aims/hypothesis—Sirtuin 6 (SIRT6) has been implicated in ageing, DNA repair and metabolism; however, its function in pancreatic beta cells is unclear. The aim of this study is to elucidate the role of SIRT6 in pancreatic beta cells.

Methods—To investigate the function of SIRT6 in pancreatic beta cells, we performed *Sirt6* gene knockdown in MIN6 cells and generated pancreatic- and beta cell-specific *Sirt6* knockout mice. Islet morphology and glucose-stimulated insulin secretion (GSIS) were analysed. Glycolysis and oxygen consumption rates in SIRT6-deficient beta cells were measured. Cytosolic calcium was monitored using the Fura-2-AM fluorescent probe (Invitrogen, Grand Island, NY, USA). Mitochondria were analysed by immunoblots and electron microscopy.

Results—*Sirt6* knockdown in MIN6 beta cells led to a significant decrease in GSIS. Pancreatic beta cell *Sirt6* knockout mice showed a ~50% decrease in GSIS. The knockout mouse islets had lower ATP levels compared with the wild-type controls. Mitochondrial oxygen consumption rates were significantly decreased in the SIRT6-deficient beta cells. Cytosolic calcium dynamics in

Corresponding author: X. C. Dong, Department of Biochemistry and Molecular Biology, Indiana University School of Medicine, 635 Barnhill Drive, MS1021D, Indianapolis, IN 46202, USA, xcdong@iu.edu.

Duality of interest: The authors declare that there is no duality of interest associated with this manuscript.

Contribution statement: XX carried out the study, interpreted and analysed the data, and wrote the manuscript. GW, RT, PW, KL, TK, XT and SAT contributed to data collection and manuscript preparation and revision. RAH, CE-M and RGM participated in the experimental design, data interpretation, and manuscript preparation and revision. W-XD contributed to data collection and interpretation and manuscript writing. XCD conceived the hypothesis, designed the experiments, analysed and interpreted the data and wrote the manuscript. XCD is the guarantor of this work. All authors approved the manuscript.

response to glucose or potassium chloride were attenuated in the *Sirt6* knockout islets. Numbers of damaged mitochondria were increased and mitochondrial complex levels were decreased in the SIRT6-deficient islets.

Conclusions/interpretation—These data suggest that SIRT6 is important for GSIS from pancreatic beta cells and activation of SIRT6 may be useful to improve insulin secretion in diabetes.

Keywords

Beta cell; Calcium; Glucose metabolism; Insulin secretion; Mitochondria; SIRT6

Introduction

The pathogenesis of type 2 diabetes is multifactorial, but impaired insulin secretion from pancreatic beta cells is one of the critical factors [1]. Glucose-stimulated insulin secretion (GSIS) is a complex process that involves glucose sensing, transport and metabolism (glycolysis and mitochondrial oxidation), plasma membrane depolarisation, and calcium signalling and exocytosis, among other things [2].

Sirtuins belong to a conserved family of proteins, and mammals have seven members (SIRT1–7) [3]. SIRT6 is a chromatin-associated enzyme that deacetylates histone H3 at lysine 9 (H3K9) and lysine 56 residues [4–6]. Some non-histone substrates, such as forkhead box O1 (FoxO1), general control of amino acid synthesis protein 5 (GCN5), and CTBP-interacting protein (CtIP), have also been reported [7–9]. SIRT6 can also remove long-chain fatty acyl groups from lysine residues of its substrates such as TNF- α [10, 11]. SIRT6-deficient mice exhibit accelerated ageing and die of hypoglycaemia by 4 weeks of age [12, 13]. SIRT6 has been implicated in a variety of metabolic processes, including glycolysis, gluconeogenesis, hepatic lipid and cholesterol metabolism, neuroendocrine regulation and circadian regulation of metabolism [7, 14–21]. Interestingly, high-fat diet (HFD)-treated *Sirt6* transgenic mice secrete more insulin in response to a bolus of glucose than their wild-type (WT) counterparts [22]. These data suggest that SIRT6 is probably required for insulin secretion and beta cell function. In this work, we generated both pancreas- and beta cell-specific *Sirt6* knockout mice to illustrate the role of SIRT6 in the pancreatic beta cells.

Methods

Animals

Pancreas-specific deletion of *Sirt6* was generated by crossing *Sirt6* floxed mice (*Sirt6*^{Tm1.1Cxd}, provided by C. Deng, Mammalian Genetics Section, National Institute of Diabetes and Digestive and Kidney Disease [NIDDK], Bethesda, MD, USA) with Tg(Pdx1-Cre)^{6Tuv} mice from the Jackson Laboratory (Bar Harbor, ME, USA) [16, 23]. Beta cell-specific *Sirt6* deletion was generated by crossing *Sirt6* floxed mice with *MIP-Cre/ERT* mice (Tg(Ins1-Cre/ERT)^{1Lphi}, provided by L. Philipson, Department of Medicine, University of Chicago, Chicago, IL, USA) and tamoxifen administration (oral gavage at a dose of 4 mg/mouse in corn oil for four consecutive days) [24]. These mice were on the mixed background (FVB/NJ:129S6/Sv:C57BL/6J). Mice were fed either regular chow (18%

energy from fat) or a HFD (42% energy from fat, Harlan Teklad, Indianapolis, IN, USA). Blood glucose levels were measured under ad libitum or overnight 16 h fasting conditions. GTT and insulin tolerance test (ITT) were performed in mice fasted for 6 h or 4 h before injection of glucose (2 g/kg, i.p. or oral gavage) or insulin (0.5 U/kg for chow-fed mice and 0.75 U/kg for HFD-fed mice, i.p.), respectively. GSIS and L-arginine-stimulated insulin secretion were performed in mice fasted for 16 h before injection of glucose (2 g/kg, i.p.) or L-arginine (1 g/kg, i.p.), respectively. Tail-vein blood samples were collected for insulin measurements using an ELISA kit (ALPCO, Salem, NH, USA). All animal procedures were performed in accordance with the National Institutes of Health (NIH) Guide for the Care and Use of Laboratory Animals and were approved by the Indiana University School of Medicine Institutional Animal Care and Use Committee. Samples were not randomised and the experimenters were not blind to group assignment and outcome assessment. No data were excluded for the report.

Cell culture

MIN6 cells (provided by D. Thurmond, Department of Pediatrics, Indiana University, Indianapolis, IN, USA) were cultured and transduced with adenoviruses as previously described [25, 26]. The cell line was verified in our laboratory and it did not have mycoplasma contamination.

Pancreatic islets

Islets were isolated from mouse pancreases at the Islet Core of the Indiana Diabetes Research Center as previously described [27].

Insulin secretion analysis

Insulin secretion analysis in MIN6 cells or mouse islets was performed as previously described [28]. Glucose, potassium chloride (KCl), α -ketoisocaproate (KIC, Sigma-Aldrich, St Louis, MO, USA) and ionomycin (IM, Cayman, Ann Arbor, MI, USA) were used for the experiments. Insulin was analysed using an ELISA kit (ALPCO).

RNA analysis

Total RNA samples were prepared and analysed as previously described [25].

Protein analysis

Protein extracts from mouse islets and other tissues or MIN6 cells were prepared and analysed as previously described [25]. The following antibodies were used: SIRT6 (Abcam, Cambridge, MA, USA, and Sigma-Aldrich, 1:1000 dilution), actinin (Santa Cruz Biotechnology, Dallas, TX, USA, 1:1000 dilution), Ac-H3K9 and cleaved caspase 3 (Cell Signaling Technology, Beverly, MA, USA, 1:1000 dilution) and total OXPHOS antibody cocktail (Abcam, 1:250 dilution). Antibodies were validated through confirmation of protein molecular weight and their known characteristics according to existing knowledge.

Histological analysis

Pancreases were fixed and processed as previously described [29]. The following antibodies were used for immunostaining: glucagon (Sigma-Aldrich, 1:5000 dilution), insulin and Ki67 (Cell Signaling Technology, 1:500 dilution). Beta cell areas were determined by analysing 10–15 pancreatic sections stained for insulin per genotype using NIH ImageJ software (<http://rsb.info.nih.gov/ij/download.html>). To examine proliferating beta cells, 15–20 islets were analysed for each genotype. The number of Ki67-positive beta cells per islet was normalised to the total beta cell number in each islet.

Pancreatic insulin content analysis

To measure total pancreatic insulin content, whole pancreas was dissected and processed as previously described [30]. Insulin was measured using an ELISA kit (ALPCO).

ATP analysis

ATP was extracted from mouse islets using 2.5% trichloroacetic acid (wt/vol.) and measured using a bioluminescent assay kit (Sigma-Aldrich).

Cellular bioenergetics analysis

The extracellular acidification rate (ECAR) and oxygen consumption rate (OCR) were measured in MIN6 cells using an XF24 Analyzer (Seahorse Bioscience, North Billerica, MA, USA).

Cytoplasmic Ca²⁺ analysis

Cytosolic Ca²⁺ dynamics in mouse islets was measured using the Fura-2-AM (Invitrogen) calcium probe as previously described [31].

Electron microscopy

Isolated mouse islets were fixed with 2% glutaraldehyde (wt/vol.) and processed as previously described [32]. Numbers of total mitochondria and damaged mitochondria from each cell were counted from a randomly selected group of 30 cells. The cytosolic area of each cell was determined using SPOT software (Sterling Heights, MI, USA), which was used to normalise the numbers of total and damaged mitochondria.

Statistical analysis

All data are presented as means \pm SEM. Two-group comparisons were performed using two-tailed unpaired Student's *t* test, and multiple-group comparisons were performed using ANOVA and Turkey's post hoc test. A *p* value of <0.05 was considered as significant.

Results

SIRT6 regulates insulin secretion from pancreatic beta cells

To examine *Sirt6* gene expression in pancreatic islets, we performed real-time PCR and western blot analysis. The mRNA levels of *Sirt6* in mouse islets were higher than that in brain, white adipose tissue, heart and liver (Fig. 1a). The western blot data also confirmed

that SIRT6 protein was more readily detectable in mouse islets than in white adipose tissue, heart and liver (Fig. 1b). It is worth noting that the SIRT6 antibodies used also detected several other bands on the blot although their identities are unknown at this time. To assess the function of SIRT6 in pancreatic beta cells, we performed knockdown of the *Sirt6* gene in a mouse insulinoma cell line, MIN6. *Sirt6* knockdown was confirmed by western blot (Fig. 1c). As expected, acetylation of the H3K9 residue, a known deacetylation substrate of SIRT6, was elevated (Fig. 1c). SIRT6-deficient MIN6 cells secreted ~30% less insulin compared with WT control cells treated with short hairpin (sh)RNAs against the green fluorescent protein gene (*shGfp*) when they were stimulated with 16.7 mmol/l glucose (Fig. 1d). These data suggest that SIRT6 regulates GSIS.

Pancreatic SIRT6 deficiency leads to insulin secretory impairment and glucose intolerance

To further investigate the physiological role of SIRT6 in pancreatic beta cell development and function, we generated *Sirt6* pancreas-specific knockout mice (bPko) by crossing mice bearing floxed *Sirt6* alleles with *Pdx1-Cre* mice. The gene knockout was very efficient as indicated by western blot and quantitative PCR analysis (Fig. 2a, b). To assess whether glucose homeostasis was perturbed in the bPko mice, we first measured blood glucose in fasting and ad libitum-fed mice. No significant difference in blood glucose levels was noticed between the control and knockout mice (Fig. 2c). However, when the bPko mice were challenged with an i.p. or oral glucose load, they showed remarkable glucose intolerance (Fig. 2d, e). The impairment in glucose tolerance can be caused by a number of factors, including insulin resistance and insulin secretory defects. ITTs did not reveal any difference between the control and bPko mice (Fig. 2f). However, plasma insulin levels (balance of secretion and clearance) were reduced under basal and glucose-stimulated states in the bPko mice (Fig. 2g). The reduction of insulin secretion can be caused by a decrease in beta cell mass, insulin content or insulin secretion. Histological analysis by haematoxylin–eosin staining and immunostaining with antibodies against insulin and glucagon did not reveal any significant difference in islet shape or size, or distribution of alpha and beta cells between the bPko and control mice (Fig. 2h, i). In addition, beta cell area and pancreatic insulin content were not significantly different (Fig. 2j, k). These data suggest that insulin secretion defects might underlie the glucose intolerance in the bPko mice.

Deletion of *Sirt6* in pancreatic beta cells causes insulin secretory defects

Although *Pdx1-Cre* has been widely used to generate pancreas-specific knockout mice, the *Cre* transgene also causes recombination in hypothalamus [24]. To investigate the role of SIRT6 in adult beta cells, we took advantage of a tamoxifen-inducible *MIP-Cre/ERT* mouse strain. The *MIP-Cre/ERT* mouse exhibits no leakage of *Cre* expression in the brain and is considered to be pancreatic beta cell-specific [24]. We first tested the knockout efficiency in the islets from *Sirt6*^{lox/lox}:*MIP-Cre/ERT* knockout (bMko) mice. *Sirt6* was efficiently deleted 2 weeks after tamoxifen administration as shown by western blot analysis and quantitative PCR of mouse islets (Fig. 3a, b). Fasting and ad libitum-fed blood glucose levels were similar in bMko, floxed (loxP) and Cre mice (Fig. 3c). However, the bMko mice showed significant glucose intolerance compared with control mice (Fig. 3d). Like the bPko mice, the bMko mice also did not exhibit any alteration in insulin tolerance (Fig. 3e).

Remarkably, the bMko mice displayed significantly lower plasma insulin levels than the control mice after a glucose load (Fig. 3f).

SIRT6 deficiency impairs mitochondrial glucose oxidation

To examine whether or not the decrease in GSIS in SIRT6-deficient islets is intrinsic to pancreatic beta cells, we performed ex vivo GSIS analysis using isolated mouse islets. Although there was no difference in insulin secretion at a low concentration of glucose (2.5 mmol/l) between bMko and control islets (Fig. 4a), the amount of insulin secreted in response to a high concentration of glucose (16.7 mmol/l) was reduced by 46% in the bMko islets compared with controls (Fig. 4a).

To identify the potential causes for the GSIS defects in SIRT6-deficient beta cells, we first examined glucose metabolism in MIN6 cells using an extracellular flux analyser (Seahorse; mouse islets could not be examined because of technical issues). Glycolysis and mitochondrial respiration can be monitored by measuring ECAR and OCR, respectively. Under high glucose conditions, *Sirt6* knockout significantly reduced the levels of ECAR and OCR in MIN6 cells, indicating a decrease of glucose metabolism (Fig. 4b, c). Next, we measured ATP production, which is the final product of mitochondrial glucose metabolism and controls insulin secretion via closure of K_{ATP} channels. At low glucose levels (2.5 mmol/l), bMko and control islets had comparable levels of ATP; however, the ATP production in response to 16.7 mmol/l glucose was decreased by ~20% in the bMko islets relative to controls (Fig. 4d). To further confirm the defect in mitochondrial energy metabolism, we used KIC, a mitochondrial substrate that can be directly metabolised by the tricarboxylic acid cycle and bypass glycolysis to perform insulin secretion assays in isolated bMko and control islets. As predicted, bMko islets secreted 58% less insulin after incubation with 12.5 mmol/l KIC compared with controls (Fig. 4e), suggesting a defect in mitochondrial oxidation.

Ablation of SIRT6 in pancreatic beta cells leads to mitochondrial defects

To examine what caused the impairment of glucose oxidation in mitochondria, we surveyed five mitochondrial complexes that are involved in the electron transport chain using a cocktail of antibodies against representative proteins from Complexes I–V. Western blots and densitometry analysis revealed that levels of Complexes III and IV were significantly decreased in the bMko mouse islets compared with controls (Fig. 5a, b). This suggests that *Sirt6* gene deletion causes mitochondrial deficiency. In order to visualise mitochondria in structural detail, we also performed transmission electron microscopy (TEM). By reviewing the TEM images, we observed noticeable mitochondrial damage in *Sirt6*-knockout beta cells (Fig. 6a–c). While total numbers of mitochondria were not different between control and SIRT6-deficient beta cells (Fig. 6d), numbers of damaged mitochondria increased in the *Sirt6*-knockout beta cells compared with the control counterparts (Fig. 6e).

SIRT6 deficiency causes aberrant calcium flux in beta cells

To further examine whether or not SIRT6 deficiency might alter membrane depolarisation and calcium flux in pancreatic beta cells, we performed insulin release analysis after L-arginine injections in mice. L-arginine is known to depolarise the plasma membrane by its

cationic charges. Plasma insulin levels were ~50% lower in the bMko mice compared with the control group 2 min after L-arginine injections (Fig. 7a). Moreover, we performed ex vivo KCl-stimulated insulin secretion in isolated mouse islets, as KCl also has a strong membrane depolarisation effect. Insulin secretion in response to 30 mmol/l KCl was decreased 50% in the bMko islets compared with the WT controls (Fig. 7b). These data suggest that the defective insulin secretion might also result from defects in either plasma membrane depolarisation and/or post-depolarisation.

In pancreatic beta cells, an increase in intracellular calcium ($[Ca^{2+}]_i$) is critical for secretagogue-induced insulin release [33, 34]. To examine whether the reduction in the insulin secretory response to glucose or KCl may be associated with reduced calcium influx, we measured $[Ca^{2+}]_i$ (indicated by the fluorescence ratio of 340 nm/380 nm) of isolated islets loaded with Fura-2-AM fluorescent probes. Consistent with the observation that bMko mice had normal basal insulin secretion, the islets from bMko and control mice showed similar resting $[Ca^{2+}]_i$ levels (Fig. 7c, d). However, in response to 16.7 mmol/l glucose or 30 mmol/l KCl, $[Ca^{2+}]_i$ was significantly lower in the bMko islets compared with the control group (Fig. 7c, d), suggesting the presence of a defect in calcium flux regulation. To further verify that the reduction of $[Ca^{2+}]_i$ is critical for the impaired insulin secretion in SIRT6-deficient beta cells, we performed insulin secretion assays in bMko and control islets in the presence of a Ca^{2+} ionophore, ionomycin. Remarkably, 30 μ mol/l ionomycin rescued the insulin secretion deficiency in the bMko islets when stimulated with 16.7 mmol/l glucose (Fig. 7e). These data suggest that SIRT6 regulates calcium flux in the pancreatic beta cells.

Pancreatic beta cell SIRT6 is required to protect mice against obesity-induced glucose intolerance

To examine the role of SIRT6 in pancreatic beta cells under obese conditions, we treated bMko and control mice with a 42% HFD for 4 months. After HFD feeding, fasting blood glucose levels were comparable between the bMko and control mice (Fig. 8a), whereas fed blood glucose levels were increased in the bMko mice although they did not reach statistical significance (Fig. 8a). Glucose intolerance was worse in the bMko mice than that in the control group (Fig. 8b). Insulin tolerance was not significantly different between the bMko and control mice (Fig. 8c). Furthermore, bMko mice exhibited greater impairment in glucose-stimulated insulin release than control mice (Fig. 8d). To investigate whether or not SIRT6 plays a role in compensatory hyperplasia of beta cells induced by the HFD feeding, beta cell area and pancreatic insulin content were analysed. There were no significant differences in the beta cell area and pancreatic insulin content between the bMko and control mice (Fig. 8e, f). Moreover, beta cell proliferation, as measured by Ki67 staining of pancreatic sections, was comparable between the bMko and control mice (Fig. 8g). In addition, analysis of cleaved caspase 3 (a marker of apoptosis) in isolated islets showed that *Sirt6* deletion did not increase caspase 3 activation even after HFD treatment (Fig. 8h).

Discussion

Impairment of GSIS is one of the early clinical manifestations in the development of type 2 diabetes [35]; however, the underlying mechanisms are not well understood. In this work,

we have shown that SIRT6 is required for proper insulin secretion in response to glucose stimulation. Our data suggest that SIRT6 regulates GSIS through mitochondrial glucose oxidation, plasma membrane depolarisation and calcium dynamics (and possibly other mechanisms).

SIRT6 is expressed in multiple tissues, albeit at different levels with high expression in the skeletal muscle, thymus and brain in mice [12]. Our data show here that SIRT6 is readily detectable in mouse islets. Data from a previous transcriptomic analysis of purified mouse pancreatic alpha and beta cells also reveal that *Sirt6* gene expression ranks in approximately the 75th and 80th percentiles among 23,406 genes in alpha and beta cells, respectively [36]. By contrast, another SIRT family member, SIRT1, which has been implicated in the regulation of insulin secretion from pancreatic beta cells [37-40], only ranks in the 68th and 64th percentiles in alpha and beta cells, respectively [36]. These data suggest that SIRT6 is likely to play a role in beta cell function.

SIRT6 has been shown to suppress glycolysis in mouse embryonic stem (ES) cells, fibroblasts and hepatocytes [16, 21]. However, this does not seem to be the case in pancreatic beta cells because glycolysis was decreased in SIRT6-deficient MIN6 cells in response to high glucose. Interestingly, the ECAR was decreased in both WT and SIRT6-deficient MIN6 cells in the presence of oligomycin, which usually inhibits mitochondrial OCR and promotes ECAR. This finding suggests that those beta cells might have low capacity to convert pyruvate to lactate compared with other cell types. Our data are consistent with a recent report in mouse primary islets [41]. It is well known that an increase in ATP levels or the ATP/ADP ratio from glucose metabolism is a critical trigger in GSIS [2]. Significantly, in our study, ATP production in the bMko islets upon glucose stimulation was lower than that in the WT islets. This result can be attributed to the compromised mitochondrial oxidation as indicated by reduced OCR in the SIRT6-deficient beta cells. Interestingly, levels of mitochondrial Complexes III and IV were decreased in the *Sirt6* knockout beta cells. The electron microscopy analysis also reveals an increase in mitochondrial damage in the SIRT6-deficient beta cells. However, the cause of the mitochondrial defects is unclear. Consistent with these findings, mitochondrial defects have been also observed in *Sirt6*-knockout mouse ES cells and *Sirt6*-knockout breast cancer cells [21, 42]. In SIRT6-deficient mouse ES cells, mitochondrial respiration and a number of intermediate metabolites in the tricarboxylic acid cycle, including citrate, isocitrate, succinate, fumarate and malate, are decreased [21]. In Hs578t breast cancer cells, overexpression of *SIRT6* increases OCR and knockout of *SIRT6* decreases it [42]. Together, these data suggest that SIRT6 promotes mitochondrial respiration. However, further study is required to elucidate how SIRT6 regulates mitochondrial function.

A high concentration of KCl can cause depolarisation of the beta cell plasma membrane, which subsequently triggers Ca^{2+} influx and insulin granule exocytosis [33]. The reduction in Ca^{2+} influx and insulin secretion from the bMko mouse islets in response to 30 mmol/l KCl seen in the current study suggests that SIRT6 may regulate insulin secretion at membrane depolarisation and/or downstream of the depolarisation event. According to our data, aberrant Ca^{2+} flux is one of the potential downstream defects in SIRT6-deficient beta cells. The first evidence is that cytosolic $[\text{Ca}^{2+}]$ was lower in bMko islets in response to high

glucose or KCl compared with the WT islets. Second, the increase of cytosolic $[Ca^{2+}]$ caused by the Ca^{2+} ionophore ionomycin normalised GSIS in the bMko islets. Since ionomycin has multiple actions that increase cytosolic $[Ca^{2+}]$, including store-operated Ca^{2+} entry and calcium-induced Ca^{2+} release [43], the precise mechanism of the regulation by SIRT6 is not clear yet. In addition, transient receptor potential cation channel, subfamily M, member 2 (TRPM2) has been suggested to play a role in insulin secretion [44, 45], and SIRT6 can modulate TRPM2 activity through its byproduct *O*-acetyl-ADP ribose (OAADPR) and its derivative ADP ribose (ADPR) [46], which can activate TRPM2 [44]. It would be interesting to see that to what extent the OAADPR/ADPR–TRPM2 pathway contributes to the SIRT6 effect on GSIS.

In summary, this work characterises the role of SIRT6 in pancreatic beta cells and reveals its importance in insulin secretion and glucose homeostasis. Specifically, our data demonstrate that SIRT6 activity is necessary to regulate insulin secretion by maintaining mitochondrial function and modulating Ca^{2+} dynamics. Therefore, it is important to further investigate the mechanisms by which SIRT6 regulates beta cell function. Pharmacological activation of SIRT6 may be useful to enhance insulin secretion and it has potential for the development of effective drugs to treat type 2 diabetes.

Acknowledgments

We thank C. Deng (NIDDK, Bethesda, MD, USA) for providing the *Sirt6* floxed mice, L. Philipson (University of Chicago, Chicago, IL, USA) for providing the *MIP-Cre* mice, D. Thurmond (Indiana University School of Medicine, Indianapolis, IN, USA) for providing the MIN6 cells, and P. Fueger, B. Maier and E. Oh (Indiana University School of Medicine, Indianapolis, IN, USA) for technical discussions.

Funding: This work was supported by grant no. R01DK091592 (XCD) from the NIDDK.

References

1. Prentki M, Nolan CJ. Islet beta cell failure in type 2 diabetes. *J Clin Invest*. 2006; 116:1802–1812. [PubMed: 16823478]
2. Prentki M, Matschinsky FM, Madiraju SR. Metabolic signaling in fuel-induced insulin secretion. *Cell Metab*. 2013; 18:162–185. [PubMed: 23791483]
3. Dong XC. Sirtuin biology and relevance to diabetes treatment. *Diabetes Manag (Lond)*. 2012; 2:243–257. [PubMed: 23024708]
4. Michishita E, McCord RA, Berber E, et al. SIRT6 is a histone H3 lysine 9 deacetylase that modulates telomeric chromatin. *Nature*. 2008; 452:492–496. [PubMed: 18337721]
5. Michishita E, McCord RA, Boxer LD, et al. Cell cycle-dependent deacetylation of telomeric histone H3 lysine K56 by human SIRT6. *Cell Cycle*. 2009; 8:2664–2666. [PubMed: 19625767]
6. Yang B, Zwaans BM, Eckersdorff M, Lombard DB. The sirtuin SIRT6 deacetylates H3 K56Ac in vivo to promote genomic stability. *Cell Cycle*. 2009; 8:2662–2663. [PubMed: 19597350]
7. Dominy JE Jr, Lee Y, Jedrychowski MP, et al. The deacetylase Sirt6 activates the acetyltransferase GCN5 and suppresses hepatic gluconeogenesis. *Mol Cell*. 2012; 48:900–913. [PubMed: 23142079]
8. Kaidi A, Weinert BT, Choudhary C, Jackson SP. Human SIRT6 promotes DNA end resection through CtIP deacetylation. *Science*. 2010; 329:1348–1353. [PubMed: 20829486]
9. Zhang P, Tu B, Wang H, et al. Tumor suppressor p53 cooperates with SIRT6 to regulate gluconeogenesis by promoting FoxO1 nuclear exclusion. *Proc Natl Acad Sci U S A*. 2014; 111:10684–10689. [PubMed: 25009184]
10. Jiang H, Khan S, Wang Y, et al. SIRT6 regulates TNF- α secretion through hydrolysis of long-chain fatty acyl lysine. *Nature*. 2013; 496:110–113. [PubMed: 23552949]

11. Feldman JL, Baeza J, Denu JM. Activation of the protein deacetylase SIRT6 by long-chain fatty acids and widespread deacylation by mammalian sirtuins. *J Biol Chem.* 2013; 288:31350–31356. [PubMed: 24052263]
12. Mostoslavsky R, Chua KF, Lombard DB, et al. Genomic instability and aging-like phenotype in the absence of mammalian SIRT6. *Cell.* 2006; 124:315–329. [PubMed: 16439206]
13. Xiao C, Kim HS, Lahusen T, et al. SIRT6 deficiency results in severe hypoglycemia by enhancing both basal and insulin-stimulated glucose uptake in mice. *J Biol Chem.* 2010; 285:36776–36784. [PubMed: 20847051]
14. Masri S, Rigor P, Cervantes M, et al. Partitioning circadian transcription by SIRT6 leads to segregated control of cellular metabolism. *Cell.* 2014; 158:659–672. [PubMed: 25083875]
15. Elhanati S, Kanfi Y, Varvak A, et al. Multiple regulatory layers of SREBP1/2 by SIRT6. *Cell Rep.* 2013; 4:905–912. [PubMed: 24012758]
16. Kim HS, Xiao C, Wang RH, et al. Hepatic-specific disruption of SIRT6 in mice results in fatty liver formation due to enhanced glycolysis and triglyceride synthesis. *Cell Metab.* 2010; 12:224–236. [PubMed: 20816089]
17. Schwer B, Schumacher B, Lombard DB, et al. Neural sirtuin 6 (Sirt6). ablation attenuates somatic growth and causes obesity. *Proc Natl Acad Sci U S A.* 2010; 107:21790–21794. [PubMed: 21098266]
18. Tao R, Xiong X, DePinho RA, Deng CX, Dong XC. FoxO3 transcription factor and Sirt6 deacetylase regulate low density lipoprotein (LDL)-cholesterol homeostasis via control of the proprotein convertase subtilisin/kexin type 9 (Pcsk9). gene expression. *J Biol Chem.* 2013; 288:29252–29259. [PubMed: 23974119]
19. Tao R, Xiong X, DePinho RA, Deng CX, Dong XC. Hepatic SREBP-2 and cholesterol biosynthesis are regulated by FoxO3 and Sirt6. *J Lipid Res.* 2013; 54:2745–2753. [PubMed: 23881913]
20. Xiong X, Tao R, DePinho RA, Dong XC. Deletion of hepatic FoxO1/3/4 genes in mice significantly impacts on glucose metabolism through downregulation of gluconeogenesis and upregulation of glycolysis. *PLoS One.* 2013; 8:e74340. [PubMed: 24015318]
21. Zhong L, D'Urso A, Toiber D, et al. The histone deacetylase Sirt6 regulates glucose homeostasis via Hif1 α . *Cell.* 2010; 140:280–293. [PubMed: 20141841]
22. Kanfi Y, Peshti V, Gil R, et al. SIRT6 protects against pathological damage caused by diet-induced obesity. *Aging Cell.* 2010; 9:162–173. [PubMed: 20047575]
23. Hingorani SR, Petricoin EF, Maitra A, et al. Preinvasive and invasive ductal pancreatic cancer and its early detection in the mouse. *Cancer Cell.* 2003; 4:437–450. [PubMed: 14706336]
24. Wicksteed B, Brissova M, Yan W, et al. Conditional gene targeting in mouse pancreatic β -cells: analysis of ectopic Cre transgene expression in the brain. *Diabetes.* 2010; 59:3090–3098. [PubMed: 20802254]
25. Xiong X, Tao R, DePinho RA, Dong XC. The autophagy-related gene 14 (Atg14). is regulated by forkhead box O transcription factors and circadian rhythms and plays a critical role in hepatic autophagy and lipid metabolism. *J Biol Chem.* 2012; 287:39107–39114. [PubMed: 22992773]
26. Kalwat MA, Wiseman DA, Luo W, Wang Z, Thurmond DC. Gelsolin associates with the N terminus of syntaxin 4 to regulate insulin granule exocytosis. *Mol Endocrinol.* 2012; 26:128–141. [PubMed: 22108804]
27. Stull ND, Breite A, McCarthy R, Tersey SA, Mirmira RG. Mouse islet of Langerhans isolation using a combination of purified collagenase and neutral protease. *J Vis Exp.* 2012
28. Fueger PT, Hernandez AM, Chen YC, Colvin ES. Assessing replication and beta cell function in adenovirally-transduced isolated rodent islets. *J Vis Exp.* 2012
29. Kono T, Ahn G, Moss DR, et al. PPAR- γ activation restores pancreatic islet SERCA2 levels and prevents beta-cell dysfunction under conditions of hyperglycemic and cytokine stress. *Mol Endocrinol.* 2012; 26:257–271. [PubMed: 22240811]
30. Antkowiak PF, Tersey SA, Carter JD, et al. Noninvasive assessment of pancreatic beta-cell function in vivo with manganese-enhanced magnetic resonance imaging. *Am J Physiol Endocrinol Metab.* 2009; 296:E573–578. [PubMed: 19116376]

31. Johnson JS, Kono T, Tong X, et al. Pancreatic and duodenal homeobox protein 1 (Pdx-1) maintains endoplasmic reticulum calcium levels through transcriptional regulation of sarco-endoplasmic reticulum calcium ATPase 2b (SERCA2b) in the islet beta cell. *J Biol Chem*. 2014; 289:32798–32810. [PubMed: 25271154]
32. Ding WX, Guo F, Ni HM, et al. Parkin and mitofusins reciprocally regulate mitophagy and mitochondrial spheroid formation. *J Biol Chem*. 2012; 287:42379–42388. [PubMed: 23095748]
33. Gilon P, Chae HY, Rutter GA, Ravier MA. Calcium signaling in pancreatic beta-cells in health and in Type 2 diabetes. *Cell Calcium*. 2014; 56:340–361. [PubMed: 25239387]
34. Yang SN, Berggren PO. The role of voltage-gated calcium channels in pancreatic beta-cell physiology and pathophysiology. *Endocr Rev*. 2006; 27:621–676. [PubMed: 16868246]
35. Weir GC, Bonner-Weir S. Five stages of evolving beta-cell dysfunction during progression to diabetes. *Diabetes*. 2004; 53(Suppl 3):S16–21. [PubMed: 15561905]
36. Benner C, van der Meulen T, Caceres E, Tigyi K, Donaldson CJ, Huising MO. The transcriptional landscape of mouse beta cells compared to human beta cells reveals notable species differences in long non-coding RNA and protein-coding gene expression. *BMC Genomics*. 2014; 15:620. [PubMed: 25051960]
37. Bordone L, Motta MC, Picard F, et al. Sirt1 regulates insulin secretion by repressing UCP2 in pancreatic beta cells. *PLoS Biol*. 2006; 4:e31. [PubMed: 16366736]
38. Luu L, Dai FF, Prentice KJ, et al. The loss of Sirt1 in mouse pancreatic beta cells impairs insulin secretion by disrupting glucose sensing. *Diabetologia*. 2013; 56:2010–2020. [PubMed: 23783352]
39. Moynihan KA, Grimm AA, Plueger MM, et al. Increased dosage of mammalian Sir2 in pancreatic beta cells enhances glucose-stimulated insulin secretion in mice. *Cell Metab*. 2005; 2:105–117. [PubMed: 16098828]
40. Pinho AV, Bensellam M, Wauters E, et al. Pancreas-Specific Sirt1-Deficiency in Mice Compromises Beta-Cell Function without Development of Hyperglycemia. *PLoS One*. 2015; 10:e0128012. [PubMed: 26046931]
41. Fu A, Robitaille K, Faubert B, et al. LKB1 couples glucose metabolism to insulin secretion in mice. *Diabetologia*. 2015; 58:1513–1522. [PubMed: 25874445]
42. Choe M, Brusgard JL, Chumsri S, et al. The RUNX2 Transcription Factor Negatively Regulates SIRT6 Expression to Alter Glucose Metabolism in Breast Cancer Cells. *J Cell Biochem*. 2015
43. Muller MS, Obel LF, Waagepetersen HS, Schousboe A, Bak LK. Complex actions of ionomycin in cultured cerebellar astrocytes affecting both calcium-induced calcium release and store-operated calcium entry. *Neurochem Res*. 2013; 38:1260–1265. [PubMed: 23519933]
44. Uchida K, Tominaga M. The role of TRPM2 in pancreatic beta-cells and the development of diabetes. *Cell Calcium*. 2014; 56:332–339. [PubMed: 25084624]
45. Yosida M, Dezaki K, Uchida K, et al. Involvement of cAMP/EPAC/TRPM2 activation in glucose- and incretin-induced insulin secretion. *Diabetes*. 2014; 63:3394–3403. [PubMed: 24824430]
46. Bauer I, Grozio A, Lasiglie D, et al. The NAD⁺-dependent histone deacetylase SIRT6 promotes cytokine production and migration in pancreatic cancer cells by regulating Ca²⁺ responses. *J Biol Chem*. 2012; 287:40924–40937. [PubMed: 23086953]

Abbreviations

ADPR	ADP ribose
bMko	<i>Sirt6</i> beta cell-specific knockout
bPko	<i>Sirt6</i> pancreas-specific knockout
[Ca²⁺]_i	Intracellular calcium
ECAR	Extracellular acidification rate
ES	Embryonic stem

GSIS	Glucose-stimulated insulin secretion
H3K9	Histone H3 at lysine 9
HFD	High-fat diet
ITT	Insulin tolerance test
KCl	Potassium chloride
KIC	α -Ketoisocaproate
NIDDK	National Institute of Diabetes and Digestive and Kidney Diseases
NIH	National Institutes of Health
OAADPR	<i>O</i> -acetyl-ADP ribose
OCR	Oxygen consumption rate
shRNA	Short hairpin RNA
SIRT6	Sirtuin 6
TEM	Transmission electron microscopy
TRPM2	Transient receptor potential cation channel, subfamily M, member 2
WT	Wild-type

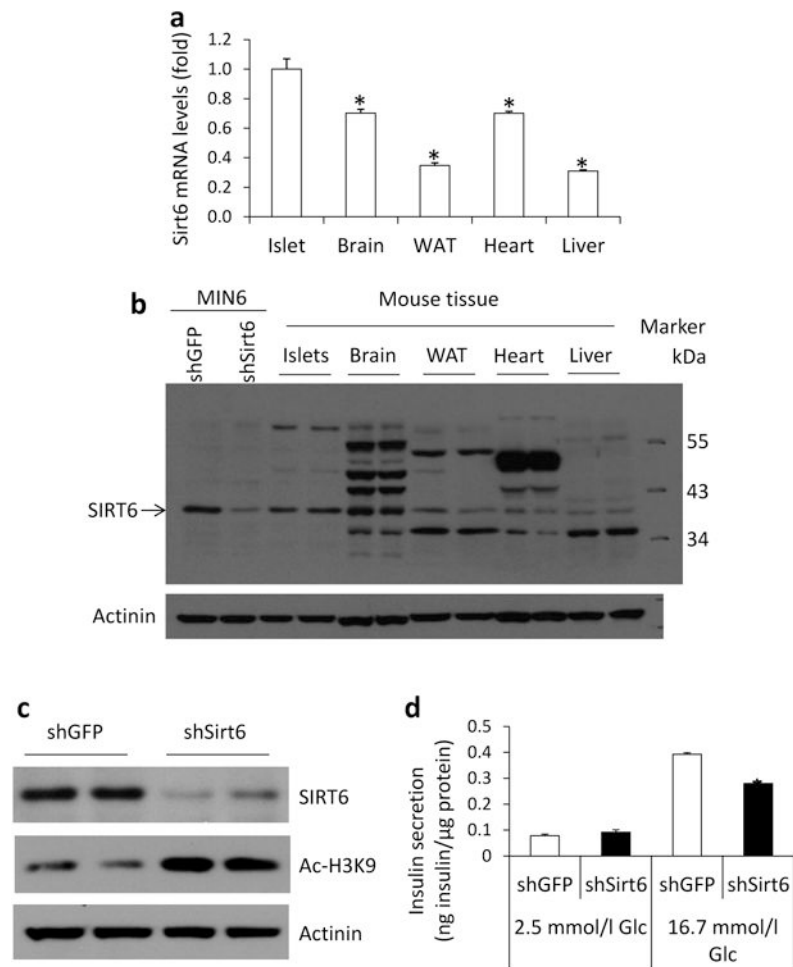


Fig. 1. *Sirt6* knockout impairs GSIS. (a) *Sirt6* mRNA and (b) SIRT6 protein analysis in WT mouse islets and other tissues. (c) Immunoblot analysis and (d) GSIS in MIN6 cells transduced with shGfp and shSirt6 shRNA-expressing adenoviruses. *Sirt6* mRNA levels in other tissues are presented as fold change to that in the islets. WAT, white adipose tissue; Glc, glucose. Data are presented as mean \pm SEM. * p <0.05 vs (a) islets; vs (d) shGfp

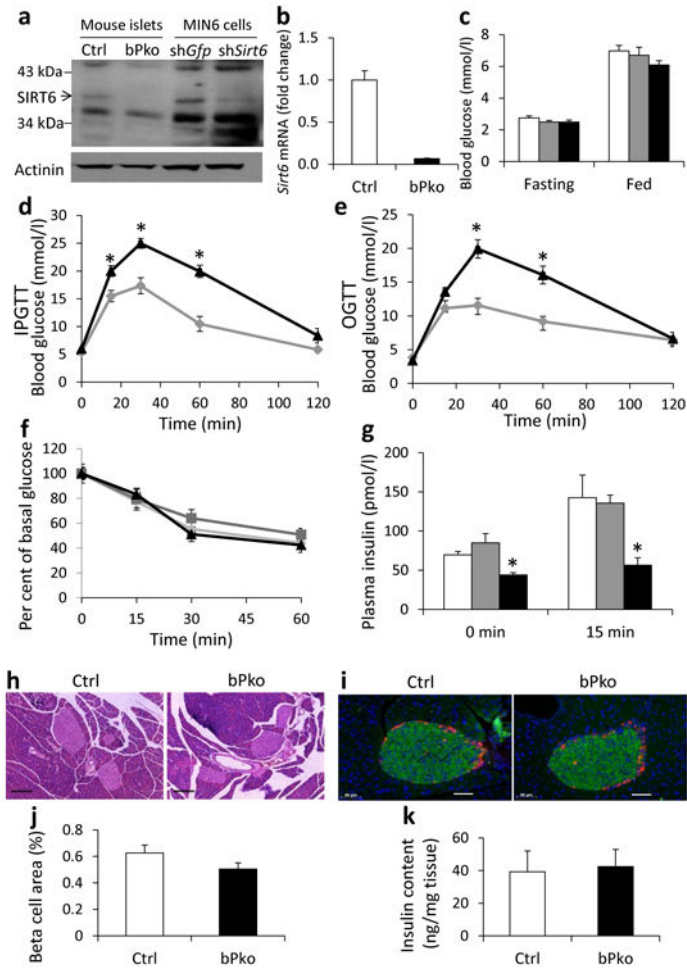


Fig. 2. Impaired glucose tolerance and GSIS in bPko mice. (a) SIRT6 protein and (b) *Sirt6* mRNA analysis in control (Ctrl) and bPko islets (MIN6 cells as controls). (c) Blood glucose, (d) i.p. GTT (IPGTT), (e) OGTT, (f) ITT and (g) GSIS in 2–3-month-old male mice ($n=6-7$ each genotype; loxp mice, white bar or light grey diamond; Cre mice, dark grey bar or square; bPko mice, black bar or triangle). Pancreatic sections stained with (h) haematoxylin–eosin and (i) insulin (green) and glucagon antibodies (red); (j) beta cell area and (k) pancreatic insulin content of control and bPko mice ($n=3$). Data are presented as mean \pm SEM. $*p<0.05$ vs Ctrl. Scale bars, (h) 100 μ m, (i) 50 μ m

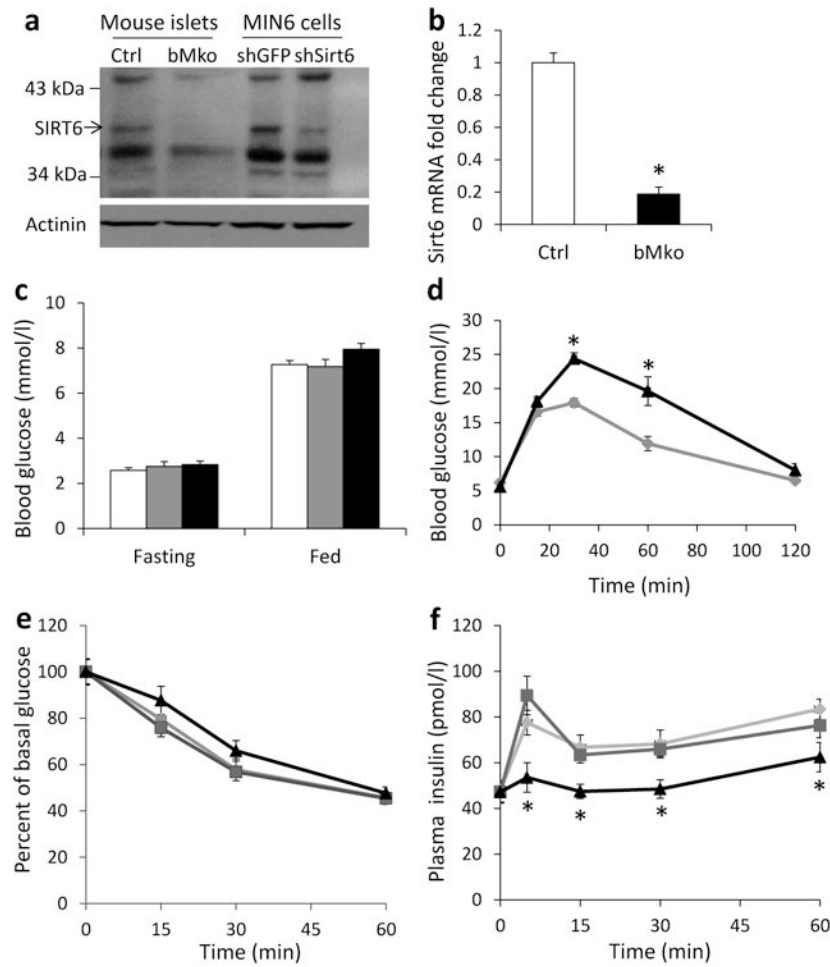


Fig. 3. *Sirt6* beta cell-specific deletion causes impaired GSIS. (a) SIRT6 protein and (b) *Sirt6* mRNA analysis in control (Ctrl) and bMko islets (MIN6 cells used as controls). (c) Blood glucose, (d) i.p. GTT, (e) ITT and (f) GSIS in 3-month-old male mice ($n=6-7$ each genotype; loxp mice, white bar or light grey diamond; Cre mice, dark grey bar or square; bMko mice, black bar or triangle). Data are presented as mean \pm SEM. * $p<0.05$ vs Ctrl

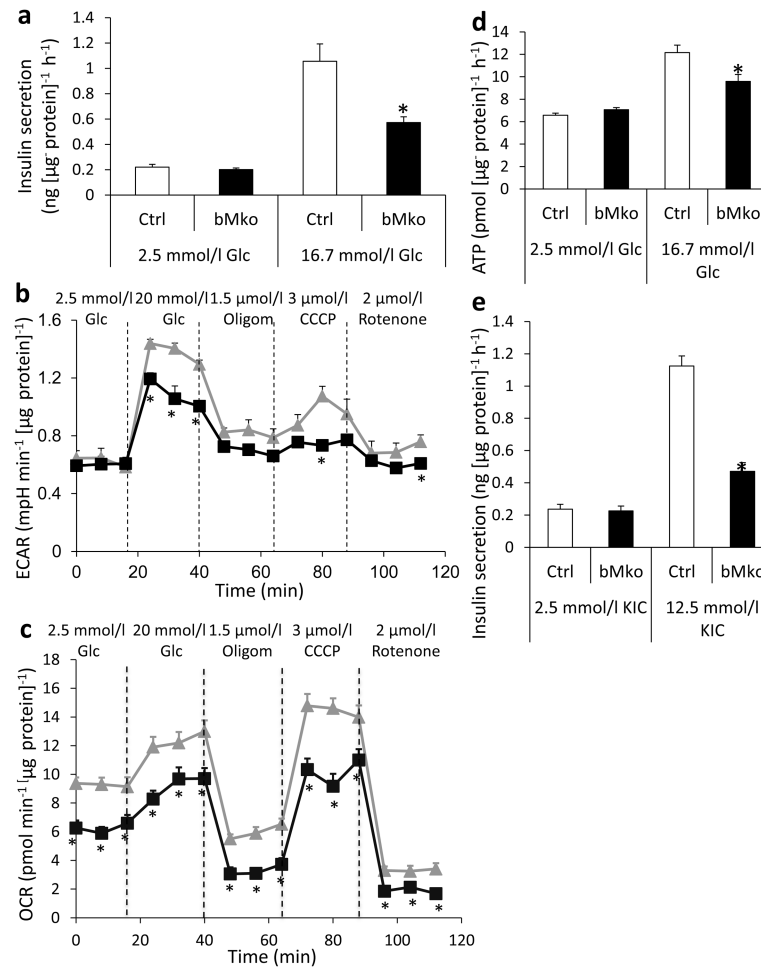


Fig. 4. SIRT6 deficiency in beta cells leads to impaired glucose oxidation. **(a)** GSIS analysis in control (Ctrl) and bMko islets. **(b)** ECAR and **(c)** OCR analysis in MIN6 cells transduced with *shGfp* (triangle) and *shSirt6* (square) adenoviruses and treated with glucose (Glc), oligomycin (Oligom), carbonyl cyanide 3-chlorophenylhydrazine (CCCP) and rotenone. **(d)** Glucose-stimulated ATP production in control and bMko islets. **(e)** KIC-stimulated insulin secretion in Ctrl and bMko islets. Each experiment was performed with pooled islets from three mice per genotype. Data are presented as mean \pm SEM, $n=3$. * $p<0.05$ vs **(a, d, e)** Ctrl, vs **(b, c)** *shGfp*

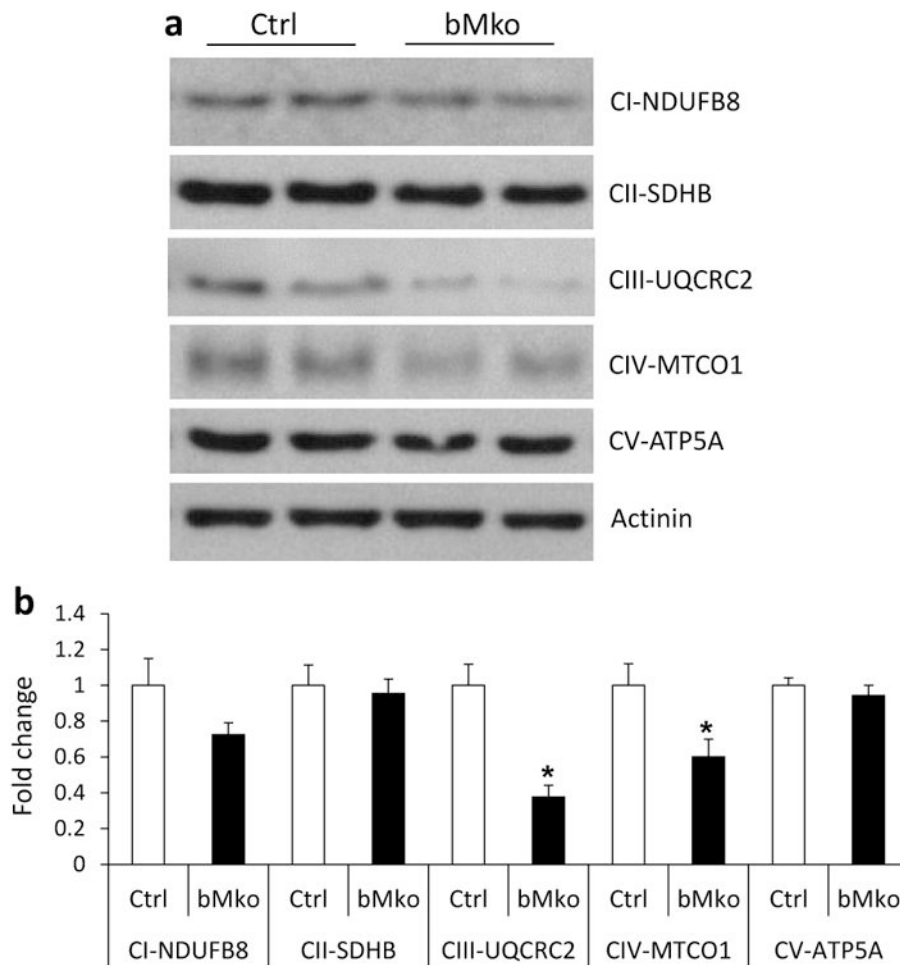


Fig. 5. Pancreatic beta cell *Sirt6* knockout leads to deficiency in the mitochondrial electron transport chain. **(a)** Immunoblot and **(b)** quantitative analysis of representative proteins in mitochondrial Complexes I–V in primary islets isolated from 4-month-old control (Ctrl) and bMko mice ($n=6$). Protein signal intensity was normalised to loading control actinin. CI-NDUFB8, Complex I-NADH dehydrogenase 1 beta subcomplex subunit 8; CII-SDHB, Complex II-succinate dehydrogenase complex subunit B; CIII-UQCRC2, Complex III-ubiquinol-cytochrome c reductase core protein II; CIV-MTCO1, Complex IV-mitochondrially encoded cytochrome c oxidase I; CV-ATP5A, Complex V-ATP synthase mitochondrial F1 complex alpha subunit. Data are presented as mean \pm SEM, $n=6$. * $p<0.05$ vs Ctrl

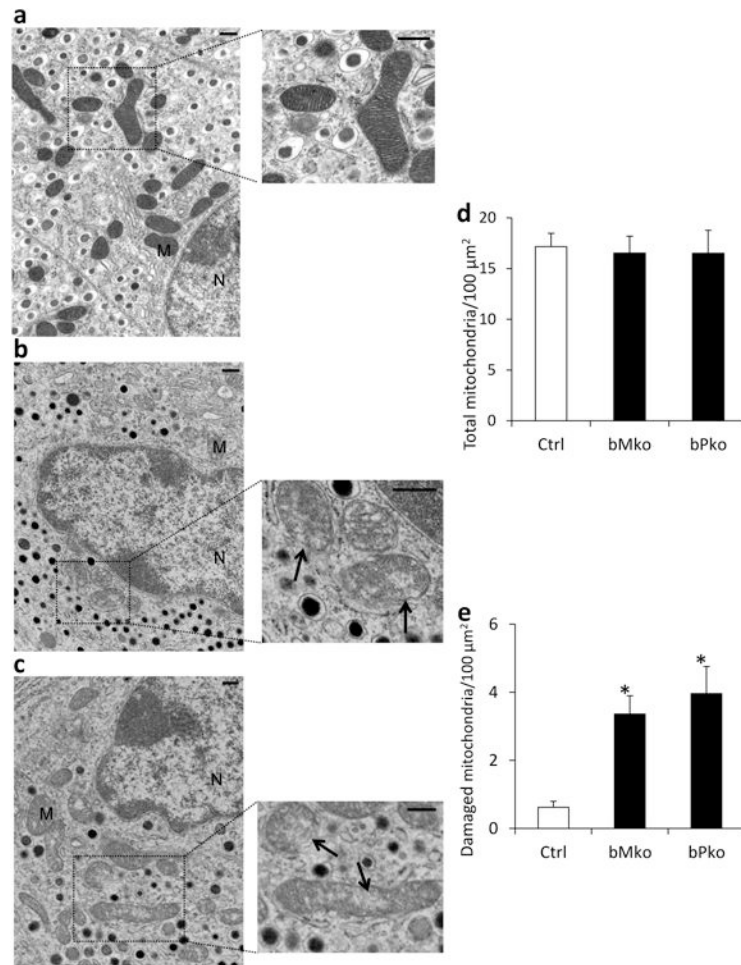


Fig. 6. Beta cell SIRT6 deficiency increases the number of damaged mitochondria. Representative electron microscopy images ($\times 3000$ magnification) of isolated islets from (a) 3-month control (Ctrl), (b) bMko and (c) bPko mice. Enlargements of areas are shown to the right. Arrows denote damaged mitochondria. Numbers of (d) total and (e) damaged mitochondria were quantified in beta cells ($n=20-30$). M, mitochondria; N, nuclei. Data are presented as mean \pm SEM. * $p < 0.05$ vs Ctrl

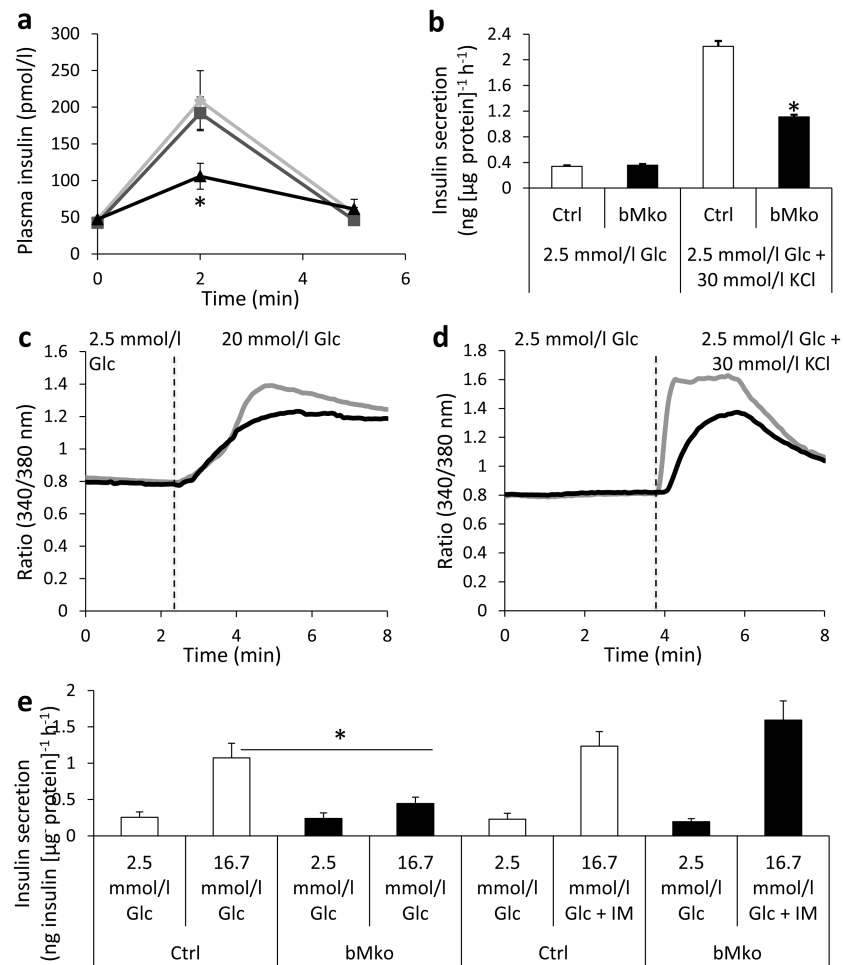


Fig. 7. Inactivation of the *Sirt6* gene in beta cells causes impaired calcium flux. L-arginine-stimulated insulin release (**a**) in 3-month-old male loxp (diamond), *MIP-Cre* (square) and bMko (triangle) mice ($n=6$ per group). KCl-stimulated insulin secretion (**b**) in (Ctrl) control and bMko islets. Representative traces of cytosolic Ca^{2+} flux measured by Fura2-AM loading in control (grey lines) and bMko (black lines) islets incubated with (**c**) glucose (Glc) and (**d**) KCl, respectively. (**e**) Insulin secretion from control and bMko islets treated with 2.5 or 16.7 mmol/l Glc alone or in combination with 30 $\mu\text{mol/l}$ ionomycin (IM). Data are presented as mean \pm SEM, $n=3$. * $p<0.05$ vs Ctrl

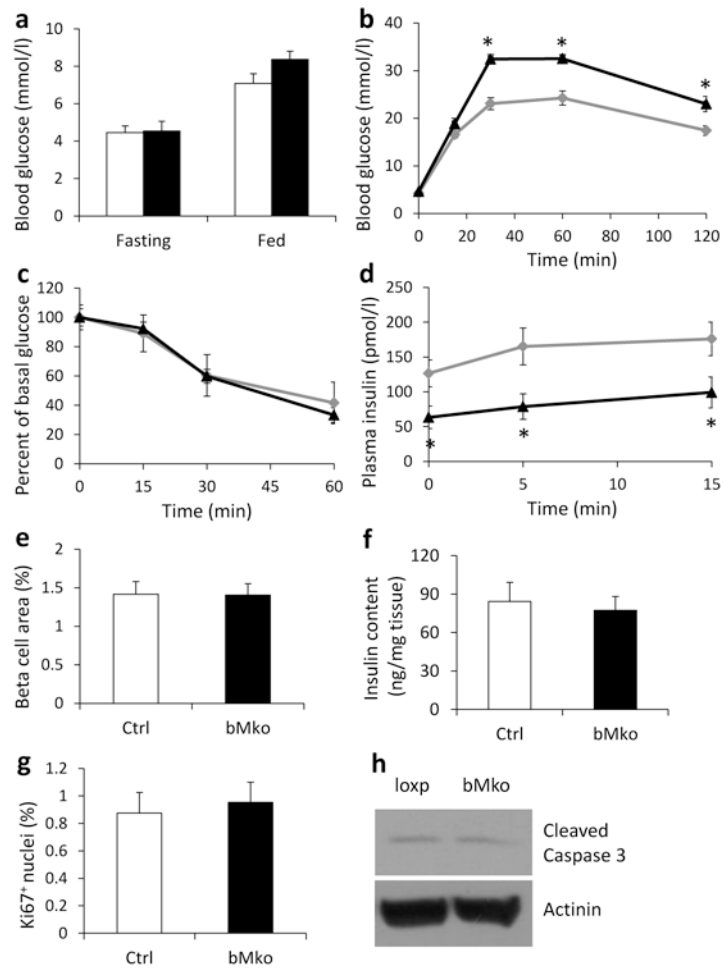


Fig. 8. Worsening of glucose intolerance and GSIS in the bMko mice on HFD. **(a)** Blood glucose, **(b)** i.p. GTT, **(c)** ITT and **(d)** GSIS in control (Ctrl, white bars/grey lines) and bMko (black bars/lines) male mice treated with 42% HFD for 3 months ($n=7-8$). **(e)** Beta cell area ($n=5$), **(f)** pancreatic insulin content ($n=5$), **(g)** Ki67-positive cells ($n=5$) and **(h)** a representative immunoblot for cleaved caspase 3 ($n=4$) Ctrl and bMko mice after 4-month HFD feeding. Data are presented as mean \pm SEM. * $p<0.05$ vs Ctrl